Direct-impact Hopkinson tests on the Ti-6Al-4V alloy at very high strain rate and inverse identification of the Johnson-Cook constitutive model

X. GUO, T. Heuzé, G. Racineux. *Research Institute in Civil and Mechanical Engineering (GeM, UMR 6183 CNRS), École Centrale de Nantes, 1 rue de la Noë, 44321 Nantes cedex 3, France Adresse(s) électronique(s) : {Xiaoli.Guo, Thomas.Heuze, Guillaume.Racineux}@ec-nantes.fr*

R. Othman. *Mechanical engineering department, Faculty Engineering, King Abdulaziz University, P.O.BOX, 80248, Jeddah, 21589, Saudi Arabia Adresse(s) électronique(s) : Ramzi.Othman@ec-nantes.fr*

Mots clés : Direct impact Kolsky bar, Inverse analysis, High strain rate, Johnson-Cook constitutive model

1 INTRODUCTION

The study of the material performance at high strain rate is an important topic in material sciences, since the materials usually exhibit strong viscous effects as the rate rises. In some material processes, the metallic materials may experience very high strain rates up to $10^6 s^{-1}$, such as the laser shock peening (Yu et al., 2009). Studying the dynamic behaviour of the materials requires to perform dynamic tests on a wide range of strain rate. The classical Split Hopkionson Pressure Bar (SHPB), also referred to as the Kolsky bar (Davies, 1948; Kolsky, 1949), is a simple device that is widely adopted to perform such dynamic tests. The classical SHPB device is capable to attain strain rates ranging from 10^2 to $10^4 s^{-1}$ (Gorham et al., 1992; Ramesh, 2008). Attempting to reach higher strain rate may yield the incident bar. Thus a direct-impact Hopkinson device has been developed (Dharan and Hauser, 1970) by removing the incident bar. On this direct-impact device, a very high strain rate of the order of $10^5 s^{-1}$ is achieved by Dharan and Hauser (1970) and Kamler et al. (1995). In this work, the Ti-6Al-4V alloy is tested on a direct-impact Hopkinson device at strain rates ranging from 3000 to $25000 s^{-1}$. Then an inverse identification is carried out to identify the Johnson-Cook model (Johnson and Cook, 1983) for the Ti-6Al-4V on this wide range of strain rates.

2 DIRECT-IMPACT TESTS ON THE TI-6AL-4V AT VERY HIGH STRAIN RATE

2.1 Design of the direct-impact configuration and experimental plan

The dynamic tests are performed on a dedicated direct-impact device which design is solution of an optimization problem as detailed in (Guo et al., 2014). This device consists mainly of a transmitted bar, the projectile and the compulsory systems for the measurement. The transmitted bar is 1.2m length and 10mm diameter. To compress the specimen on a wide range of strain rate, four projectiles are manufactured, of diameter 15.8mm and lengths of 500mm, 125mm, 60mm and 30mm respectively. The bar and the projectiles are all made of a high strength steel, MARVAL X2NiCoMo18-8-5, with a yield stress of 1800MPa. Three Wheastone bridges of double gauges are mounted along the bar length to measure the elastic strain and monitor the dispersion. Two laser diodes are equipped to measure the impact velocity of the projectile. A high speed camera is also equipped to observe the compression of the specimen and the movement of the projectile during the impact.
The experimental plan comes down to determine the value of the specimen length l_s, the projectile length l_p and its impact velocity v_p. However, the combination of these three parameters is not unique to get a given strain rate. Provided the expected strain rate $\dot{\varepsilon}_s$ and the allowable strain ε_s in the specimen, their maximum values can be approximated through the following equations, c_p being the sound speed in the projectile :

$$\dot{\varepsilon}_{s_{\max}} \approx \frac{v_p}{l_s} \quad , \qquad \varepsilon_{s_{\max}} \approx \dot{\varepsilon}_s \frac{2l_p}{c_p} \tag{1}$$

The combination of the parameters for each objective strain rate is presented in table 1.

TABLE 1 – Experimental plan and results

Test n°	Obj. $\dot{\varepsilon}$ (s^{-1})	v_p (m/s)	l_p (mm)	l_s (mm)	$\dot{\varepsilon}_{\max}$ (s^{-1})	$\varepsilon_{\max}$	Test n°	Obj. $\dot{\varepsilon}$ (s^{-1})	v_p (m/s)	l_p (mm)	l_s (mm)	$\dot{\varepsilon}_{\max}$ (s^{-1})	$\varepsilon_{\max}$
T1	3000	15	500	5	3064	11%	T7	18000	36	60	2	17970	33%
T2	5000	25	125	5	4642	16%	T8	18000	30	60	1.5	18350	16%
T3	7000	28	125	4	6925	17%	T9	20000	30	60	1.5	21222	23%
T4	10000	30	60	3	10740	17%	T10	20000	40	30	2	19659	24%
T5	12000	36	60	3	12040	25%	T11	25000	37.5	30	1.5	25050	25%
T6	15000	30	60	2	15010	11%							

2.2 Measurements from the direct-impact tests

The measured data consist of the elastic strain $\varepsilon_b(t)$ in the transmitted bar and the impact velocity v_p of the projectile. The force $F_s(t)$ applied by the bar on the specimen is computed from the recorded strain $\varepsilon_b(t)$:

$$F_s(t) = E_b S_b \varepsilon_b(t) \tag{2}$$

where E_b and S_b are the Young's modulus and the cross-section of the bar. The force $F_s(t)$ computed for the tests listed in table 1 is plotted in the figure 1 for each projectile length. In these curves, some trays are observed during the unloading part. These arise from (i) the shorter length of the projectile than that of the bar and (ii) the mismatch of the *generalized wave impedances* (Wang, 2007) of the projectile $(\rho c S)_p$, the specimen $(\rho c S)_s$ and the transmitted bar $(\rho c S)_b$. Moreover, when the projectile is long enough, the loading time is equivalent to the characteristic time, as shown in the figure 1(a) where the projectile is 500mm length. As the projectile length shortens, the actual period of the compression of the specimen lasts approximately twice the characteristic time or even longer as observed in the figures 1(b)-1(d). This results from the different cross-sections of the projectile and the bar in these experiments.

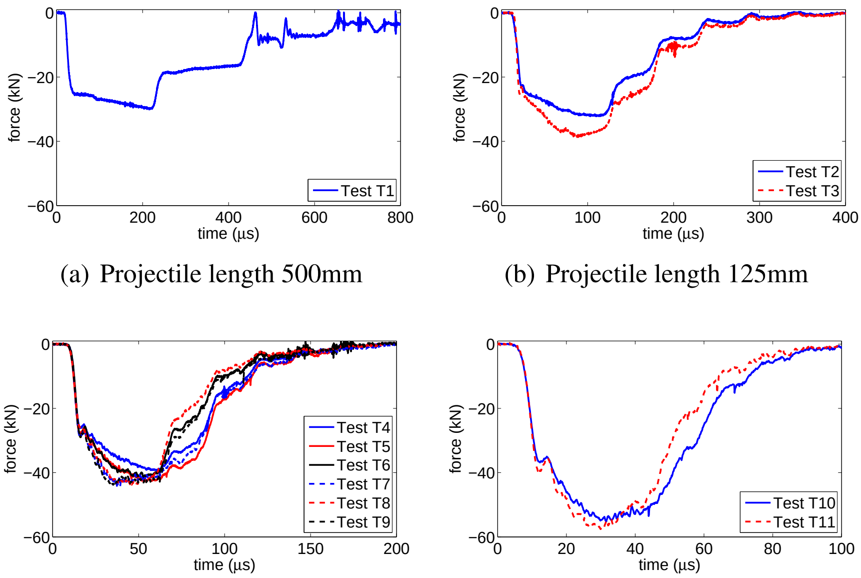

(a) Projectile length 500mm

(b) Projectile length 125mm

(c) Projectile length 60mm

(d) Projectile length 30mm

FIGURE 1 – Force on the specimen in the direct-impact tests

Without any input bar to measure the input force, the strain rate in the specimen is assessed by the following equation (Gorham et al., 1992; Guo et al., 2014) :

$$\dot{\varepsilon}_s(t) = -\frac{v_p + \frac{S_p + S_b}{S_p} c_b \varepsilon_b(t)}{l_s} \tag{3}$$

where S_p and c_b are the cross-section of the projectile and the sound speed of the bar. The maximum compressive strain rate $\dot{\varepsilon}_{\text{max}}$ assessed by this equation and the measured compressive strain ε_{max} are presented in table 1 for each test. According to this formula, the compressive strain rate gets its extremum equal to v_p/l_s at the beginning of the impact. However, this equation is only valid within the characteristic time (Gorham et al., 1992).
Since the force equilibrium of the specimen can not be checked, and the actual loading period is much longer than the characteristic time, an inverse analysis is carried out to identify the dynamic behaviour of the Ti-6Al-4V alloy.

3 INVERSE IDENTIFICATION OF THE JOHNSON-COOK CONSTITUTIVE MODEL

A constitutive model is first postulated to describe the behaviour of the tested material. The parameters of this constitutive model are then identified so that some given quantities extracted from the numerical simulation fit experimental data. The Johnson-Cook model is widely adopted to describe the dynamic behaviour of metallic materials, and is here used for the Ti-6Al-4V alloy. The temperature effects are not addressed in this work, the Johnson-Cook equation thus reads :

$$\sigma(\varepsilon^p_{eq}, \dot{\varepsilon}^p_{eq}) = \left(A + B(\varepsilon^p_{eq})^n\right)\left(1 + C \ln \frac{\dot{\varepsilon}^p_{eq}}{\dot{\varepsilon}_0}\right) \tag{4}$$

The parameters A, B and n are identified on quasi-static stress-strain curves obtained at the strain rate of $10^{-4}s^{-1}$: A=955MPa, B=770MPa and n=0.557. A reasonable range of search of $0.005 \leq C \leq 0.05$ is set for the parameter C. Then a 2D axisymmetric finite element model is established in ABAQUS to run the inverse analysis in order to identify the parameter C. The cost function $f(\mathbf{x})$ is defined as the euclidean norm of the difference between the simulated strain $\varepsilon_{\text{sim}}(\mathbf{x}, t)$ extracted at the location of the gauge and the recorded one $\varepsilon_{\text{exp}}(t)$.

$$f(\mathbf{x}) = \parallel \varepsilon_{\text{sim}}(\mathbf{x}, t) - \varepsilon_{\text{exp}}(t) \parallel_2 \tag{5}$$

The figure 2 presents the superposed plots of the recorded and calibrated strain curves of some tests, and also shows the values of C identified on each test with respect to the experimental strain rates assessed by equation 3. In the figures 2(a)-2(c), the calibrated strain curves fit well the recorded ones

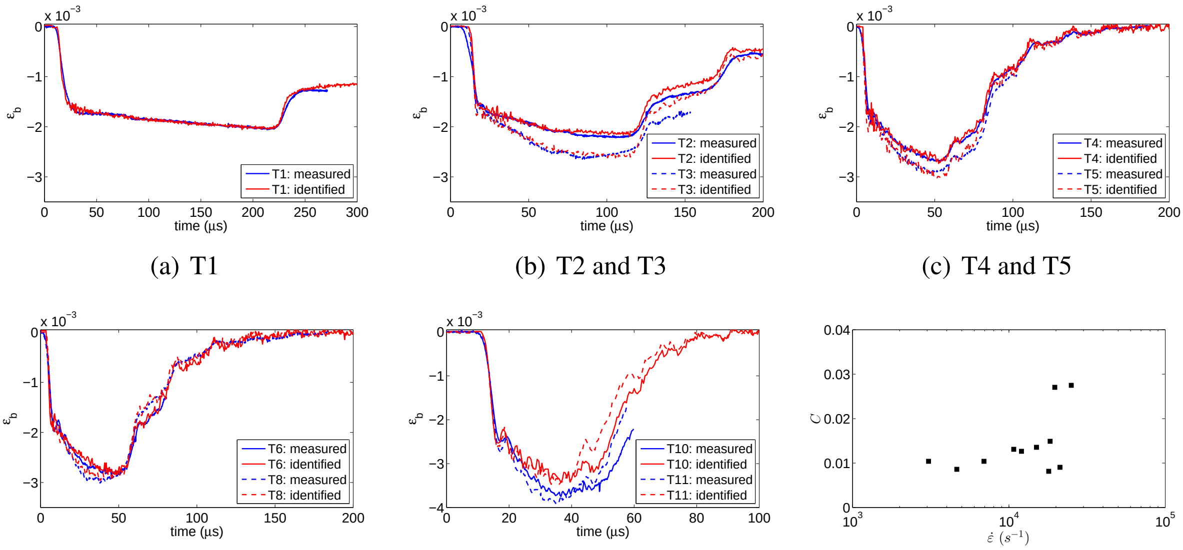

(a) T1 (b) T2 and T3 (c) T4 and T5

(d) T6 and T8 (e) T10 and T11 (f) Identified C

FIGURE 2 – Recorded and calibrated strain curves

in the loading stage. However some discrepancies can also be observed during the unloading period. In the figure 2(d), slight discrepancies appear in the loading stage, when the strain rates exceed 10^4s^{-1}. This kind of discrepancies increases as the strain rate goes beyond $20000s^{-1}$ as shown in the figure 2(e). In the figure 2(f), the parameter C is almost constant in the range of 3000 to $15000s^{-1}$. As the strain rate increases, the results of the identification are subject to more scattering. A much greater value of C of about 0.03 is obtained when the strain rate is over $20000 s^{-1}$, whereas a smaller one is identified on the tests T7 and T9. For many ductile materials, it has been observed that the stress increases more rapidly as the strain rates excess the level of $10^3 s^{-1}$(Rule and Jones, 1998). However here, more tests and identifications are required to come to a reliable conclusion for the highest strain rates.

4 CONCLUSION

In this work, the Ti-6Al-4V has been tested on the direct-impact Hopkinson device on a wide range of strain rate ranging from 3000 to $25000 s^{-1}$. Due to the mismatch of the material impedances and cross-sections, a longer loading period has been observed in the force curves. Thus an inverse identification procedure has been adopted to identify the Johnson-Cook model for the Ti-6Al-4V on the experimental data. It has been shown that this model works well at least up to $20000 s^{-1}$, even though more tests are required for strain rates greater than this value.

Références

Davies, R. M. (1948). A critical study of the Hopkinson Pressure Bar. *Philosophical Transactions of the Royal Society of London. Series A. Mathematical and Physical Sciences*, 240(821) :375–457.

Dharan, C. K. H. and Hauser, F. E. (1970). Determination of stress-strain characteristics at very high strain rates. *Experimental Mechanics*, 10(9) :370–376.

Gorham, D. A., Pope, P. H., and Field, J. E. (1992). An improved method for compressive stress-strain measurements at very high strain rates. *Philosophical Transactions of the Royal Society of London. Series A. Mathematical and Physical Sciences*, 438(A) :153–170.

Guo, X., Heuzé, T., Othman, R., and Racineux, G. (2014). Inverse identification at very high strain rate of the Johnson-Cook constitutive model on the Ti-6Al-4V alloy with a specially designed direct-impact Kolsky bar device. *Strain*, 50(6) :527–538.

Johnson, G. R. and Cook, W. H. (1983). A constitutive model and data for metals subjected to large strains, high strain rates and high temperatures. *Proceedings of the 7th International Symposium on Ballistics*, pages 541–547.

Kamler, F., Niessen, P., and Pick, R. J. (1995). Measurement of the behaviour of high-purity copper at very high rates of strain. *Canadian Journal of Physics*, 73(5–6) :295–303.

Kolsky, H. (1949). An investigation of the mechanical properties of materials at very high rates of loading. *Proceedings of the Physical Society. Section B*, 62.

Ramesh, K. T. (2008). Part D : Chapter 33. High strain rate and impact experiments. In *Springer handbook of experimental solid mechanics*, pages 1–31. Springer.

Rule, W. K. and Jones, S. E. (1998). A revised form for the Johnson-Cook strength model. *International Journal of Impact Engineering*, 21(8) :609–624.

Wang, L. (2007). *Foundations of stress waves*. Elsevier Science.

Yu, C., Gao, H., Yu, H., Jiang, H., and Cheng, G. J. (2009). Laser dynamic forming of functional materials laminated composites on patterned three-dimensional surfaces with applications on flexible microelectromechanical systems. *Applied Physics Letters*, 95(9) :091108.